Uni-Planar CPW-Fed Slot Launchers for Efficient TM_0 Surface-Wave Excitation

Hany F. Hammad, Yahia M. M. Antar, *Fellow, IEEE*, Al P. Freundorfer, *Member, IEEE*, and Samir F. Mahmoud, *Senior Member, IEEE*

***Abstract*—Several new uni-planar coplanar-waveguide-fed slot surface-wave launchers are presented in this paper. The launchers are used to efficiently excite the dominant transverse-magnetic surface-wave mode inside a grounded dielectric slab for possible use in power combiners and other applications. Analysis of the surface waves and optimization of the slab thickness and other needed parameters are presented. Next, the launchers design and optimization using two commercially available software are described. The launchers were fabricated and tested. Good agreement is obtained between the numerical and experimental results.**

***Index Terms*—Power combiners, surface-wave launchers, Yagi–Uda coplanar slot antennas.**

I. Introduction

SURFACE-WAVE excitation and propagation properties play an important role in several antennas and millimeter-wave integrated-circuit applications. In some of these applications, the goal of the surface-wave optimization is to suppress these surface waves (e.g., microstrip antenna arrays). On the other hand, during the last decade, several new applications have emerged. In these applications, the surface-wave excitation and propagation properties need to be controlled to serve specific uses. One such application is the implementation of quasi-optical slab beam power combiners [1]–[3]. Quasi-optical power combiners have become more attractive in recent years in view of the several advantages they offer over transmission-based combiners [4]. One type of these quasi-optical power combiners is the slab-beam type, in which the power feeding and excitation is done inside the slab by using its dominant mode [1]–[3]. Accordingly, to achieve efficient combining, the excitation of the dominant mode should be maximized and directed. Slot antenna launchers are the favorite candidates for TM_0 excitation. This is due to the fact that a half-wavelength slot in a ground plane has an E-field that can match the E-fields of the dominant mode of the slab. In the literature, slots were commonly fed by rectangular waveguides [5] and microstrip transmission lines [2]. Both feeding techniques need circuits that are not compatible with monolithic fabrication techniques. Furthermore, these waveguide or microstrip-based circuits are very difficult to realize at millimeter-wavelength frequencies. In this paper, several new quasi-Yagi–Uda coplanar-waveguide (CPW)-fed slot launcher configurations are presented. The newly developed launchers are employed to achieve efficient and directed surface-wave excitation. Feeding the slot with a CPW offers the advantage of achieving a uni-planar structure (a one metallic layer), which is compatible with monolithic fabrication techniques [6]. To achieve the directed excitation, a Yagi–Uda-like technique is developed. In this technique, parasitic slots with lengths shorter than the driven slot (directors) or longer than the driven slot (reflectors) are placed in close proximity to the driven slot to achieve the directive radiation [7]. The newly developed launchers include a director-based configuration, reflector-based configuration, and a combination of both reflector- and director-based configurations. To optimize the launchers performance, two different software packages were employed. These packages are *IE3D* (method of moments-based software by Zeland Software, Fremont, CA), and *HFSS* (finite-element-based software by the Ansoft Corporation, Pittsburgh, PA). The agreement obtained through the use of two different numerically based software provided confidence in the obtained results.

The optimization of the slab parameters and the supported surface waves is initially presented in Section II. This is followed by the details of the design of each of the newly developed launchers in Section III. To verify the theory, two sets of launchers were fabricated and tested, the first at 30 GHz and the second at 12 GHz.

II. Slab-Beam Thickness Optimization

As mentioned earlier, slot-based launchers are the favorite candidates for TM_0 excitation. This is due to the fact that a half-wavelength slot in a ground plane has an E-field that can be efficiently coupled to the E-fields of the dominant mode of the slab [10]. Due to the fact that the surface wave will be launched in the grounded slab from a slot etched in the ground plane, the slab thickness and dielectric constant (ε_r) must be carefully chosen to ensure the following.

1) Launching of the dominant slab mode (TM_0) only, this is due to the fact that overmoding the slab will result in power loss in the higher order modes ($\mathrm{TE}_1, \mathrm{TM}_1, \ldots,$ etc.).
2) Maximizing the ratio between the slot excited surface-wave power and the slot radiated power. This is

Manuscript received July 11, 2002; revised November 6, 2002. This work was supported by the Natural Sciences and Engineering Research Council of Canada, by Communication and Information Technology Ontario, by the Royal Military College, and by Queen's University.

H. F. Hammad and A. P. Freundorfer are with the Electrical and Computer Engineering Department, Queen's University, Kingston, ON, Canada K7L 3N6.

Y. M. M. Antar is with the Electrical and Computer Engineering Department, Royal Military College of Canada, Kingston, ON, Canada K7K 7B4.

S. F. Mahmoud is with the Electrical Engineering Department, Kuwait University, Safat 13060, Kuwait.

Digital Object Identifier 10.1109/TMTT.2003.809668

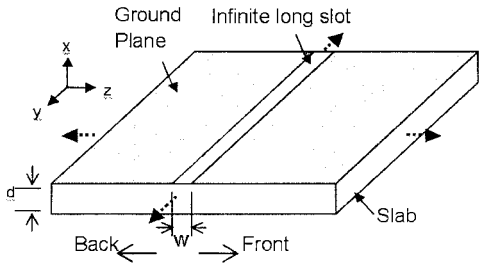

Fig. 1. Configuration of the slot on an infinite size grounded dielectric slab.

due to the fact that the slot radiated power represents undesired leakage.

3) Avoiding the operation close to or above the leakage cutoff frequency of the CPW. Operation above the leakage cutoff frequency will result in power loss and crosstalk [8], [9].

Consequently, the first step is to ensure that only the dominant slab beam mode is propagating inside the slab. The total number of surface-wave modes supported by a guide of given permittivity and thickness is equal to the largest integer (N) satisfying the condition [1]

$$N < \frac{k_o d}{\pi}\sqrt{\varepsilon_r - 1} \tag{1}$$

where d is the slab thickness, $k_0 = \omega\sqrt{\mu_0\varepsilon_0}$ is the surface-wave wavenumber, and ε_r is the relative dielectric constant of the slab. Thus, to ensure the excitation of only TM_0, the value of N in (1) should be less than 1. For instance, for operation below TM_1 for a slab made of alumina $(\varepsilon_r = 9.8)$, the ratio d/λ_0 should be less than 0.1685, i.e., $d = 1.685$ mm at 30 GHz.

The second step of the dielectric slab optimization is to choose the slab thickness and permittivity so that the surface-wave excitation is maximized. For this purpose, a theoretical derivation of surface-wave power and radiation from a two-dimensional model of a grounded dielectric slab has been undertaken by the authors [11]–[13]. The slab is assumed to be excited by a magnetic line source that represents the fields in a narrow y-oriented slot in the ground plane, as shown in Fig. 1. For a voltage V_{slot} applied across the slot, the magnetic line source carries an equivalent magnetic current $M_y = V_{\mathrm{slot}}$ that generates surface-wave modes traveling in both the $+z$- and $-z$-directions. In addition, radiation, or leakage fields, are produced in both directions as well. Using the transverse spectral representation of the fields, both surface wave (P_{sw}) and leakage power (P_{leakage}) per meter along y (the line-source orientation) can be defined [12] as

$$P_{\mathrm{sw}} = \frac{M_y^2}{2}\sum_n [N_n]^{-1} \tag{2}$$

$$P_{\mathrm{leakage}} = \frac{M_y^2}{2}\int_0^{k_0} [N(k_x)]^{-1} dk_x. \tag{3}$$

The summation in (2) is over the finite number of allowable TM surface waves. This is usually limited to one surface-wave mode. The integration in (3) is over the transverse wavenumber k_x, and the factors N_n and $N(k_x)$ are given by

$$N_n = \frac{\beta_n}{\omega\varepsilon_0}\left[\frac{d}{2\varepsilon_r}\left(1 + \frac{\sin(2g_n d)}{2g_n d}\right) + \frac{\cos^2(g_n d)}{2\sqrt{\beta_n^2 - k_0^2}}\right] \tag{4}$$

$$N(k_x) = \frac{\pi\sqrt{k_0^2 - k_x^2}}{2\omega\varepsilon_0 k_x^2 \varepsilon_r^2}\left[k_x^2\varepsilon_r^2\cos^2(gd) + g^2\sin^2(gd)\right] \tag{5}$$

where $g_n = \sqrt{\varepsilon_r k_0^2 - \beta_n^2}$, $g = \sqrt{\varepsilon_r k_0^2 - k_x^2}$, and $k_0 = \omega\sqrt{\mu_0\varepsilon_0}$, while β_n is the longitudinal phase constant of the nth surface-wave mode.

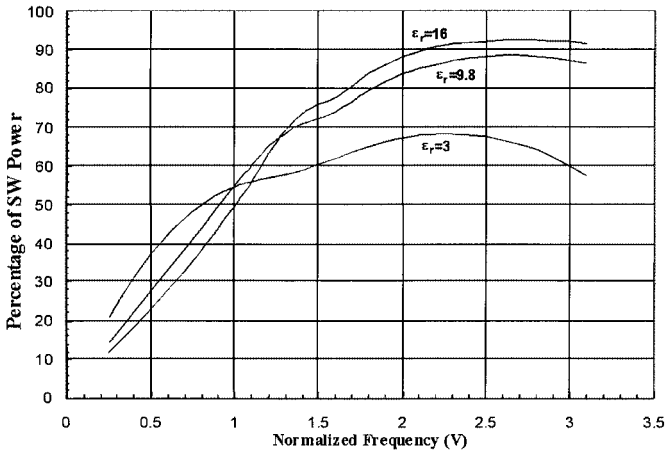

Fig. 2. Percentage of surface-wave power launched by a slot on a grounded dielectric slab versus normalized frequency for $\varepsilon_r = 3$, 9.8, and 16.

The percentage surface-wave power launched by the assumed infinite slot can be computed from (2) and (3) and is thus plotted in Fig. 2 as a function of the normalized frequency parameter $V = k_0 d\sqrt{\varepsilon_r - 1}$. The relative dielectric constant ε_r is taken as a parameter with $\varepsilon_r = 3.0$, 9.8, and 16. We limit V to values less than π for a single surface-wave-mode operation. It can be concluded from Fig. 2 that the maximum percentage of surface-wave power increases as ε_r increases. It is seen that, for a relative dielectric constant around 9.8, the maximum-percentage surface-wave power occurs at $V \approx 2.5$. The slot conductance can also be computed from (2) and (3) by using the simple formula

$$G_{\mathrm{slot}} = \frac{\lambda_0\left[P_{\mathrm{sw}} + P_{\mathrm{leakage}}\right]}{M_y^2}. \tag{6}$$

It is to be noted that the units of G_{slot} is siemens/λ_0, or siemens per free-space wavelength along the slot. G_{slot} is plotted versus V in Fig. 3, where it displays a peak at $V \approx 1.6$ and the peak value increases with the substrate ε_r. Accordingly, the operating frequency should be a tradeoff between $V = 1.6$ and $V = 2.5$ as a compromise between maximum conductance and maximum percentage surface-wave power.

Finally, since the launchers are CPW based, the launcher design frequency should be below the CPW leakage cutoff frequency (f_c) [8], [9]. Accordingly, V was chosen to be equal to 1.9. As an example, for a 2.54-mm-thick RT/Duroid $(\varepsilon_r \cong 10)$, operation should be below $V = 1.9$ (frequency of 12 GHz), as indicated in Fig. 4. In this case, approximately 82% of the power delivered by the slot antenna is guided as a surface wave. The

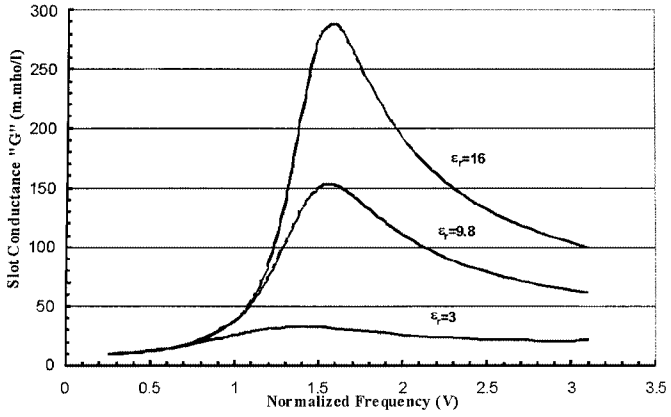

Fig. 3. Slot conductance per a free-space wavelength λ_0 along y V.

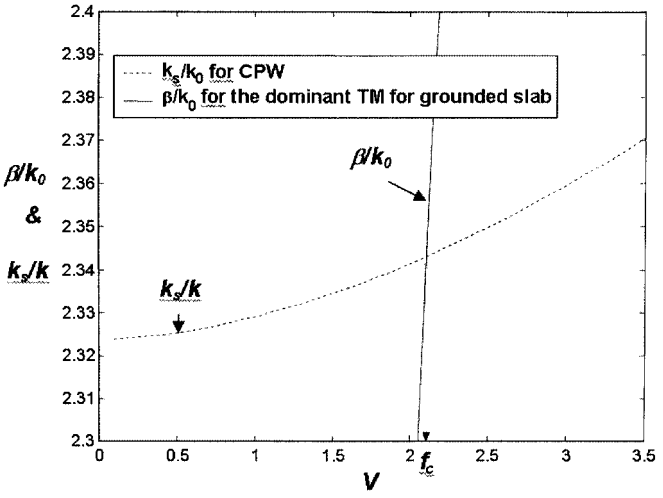

Fig. 4. Determining the cutoff frequency (f_c) in the leakage analysis of CPW over alumina substrate by the intersection of CPW dispersion characteristic, and the grounded slab dominant mode.

remaining 18% is in radiated power. However, the surface-wave power is not directed, and an equal amount of power will be directed in both the front and back directions, as shown in Fig. 1. Accordingly, to achieve directed radiation, parasitic slots will be used. The analysis and design of the directed launcher are going to be presented in detail in Section III.

III. CPW-Fed Surface-Wave Launchers

As previously discussed, the grounded slab thickness was optimized for maximum surface-wave power excitation. However, the excitation is not directed and, hence, half the power is lost in the back direction. Accordingly, in this section, several directed TM_0 surface-wave launchers are presented. In this study, the slot will be fed using a CPW etched in the same ground plane of the slot. Hence, compared to a microstrip-fed slot [3], a CPW-fed slot offers a compact and uni-planar (only one metallic layer) structure that is compatible with monolithic-microwave integrated-circuit (MMIC) fabrication. To force the excitation in one direction, a Yagi–Uda-like concept will be introduced. The launchers presented include reflector-, director-, and director–reflector-based structures.

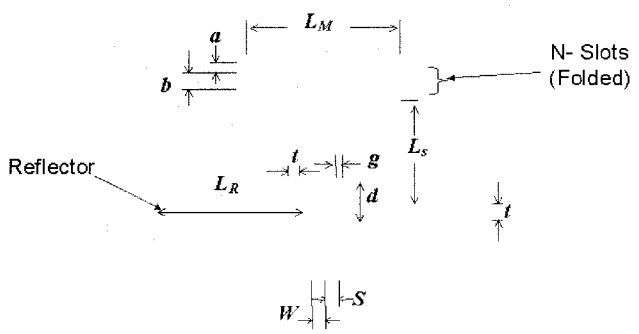

Fig. 5. Configuration of the reflector-based launcher.

A. Reflector-Based Launcher

As the name implies, the launcher presented in this section achieves its directivity using a reflector-based Yagi–Uda concept. In this section, the configuration and concept of the launcher, together with the numerical and experimental verifications, will be presented.

Configuration: In a Yagi–Uda array, a parasitic reflector antenna element is positioned close to the driven antenna element so that the magnetic current on the parasitic element leads the driven antenna with a 90° phase shift. Consequently, toward the driven antenna element, the fields add constructively. On the other hand, toward the reflector antenna element, the fields add destructively. Accordingly, the fields are directed in the direction of the driven antenna. The overall array directivity or forward/backward ratio (FBR) can be defined as the ratio of the forward (toward the driven antenna element) and backward field values (toward the parasitic reflector antenna element). The obtained directivity can be maximized by optimizing the spacing between the two elements and the length of the reflector antenna element.

Generally, a Yagi–Uda reflector-based launcher should have a single reflector. Due to the fact that the structure employed here is CPW fed, the feeding network will be etched on the same plane as the two slots (driven and reflector slots). Hence, the implementation of the reflector-based configuration has proven to be a challenging task. The developed configuration is shown in Fig. 5. The configuration is a two half-wavelength inductively coupled slot reflector instead of a single half-wavelength slot reflector [14]. The inductive coupling terminology is used to emphasize that the coupling between the CPW and slot is achieved through the magnetic field [15]. The magnetic fields, excited by the electrical currents in the spacing between the CPW and slot, induce electric fields inside the slot. Since the electrical fields in the portions of the slots of length "d" are oppositely directed, the fields cancel and do not contribute to the surface-wave excitation. The reflectors appear as a series load with the CPW feed line. The lengths g and d were adjusted to achieve low inductive coupling to ensure that the two reflector slots almost behave as parasitic elements to the driven slot. The input impedance of the launcher was matched to 50 Ω by using the folded-slot approach described in [16], where it was shown that the folded-slot technique indicates that the input impedance of N folded slots (Z_{in})

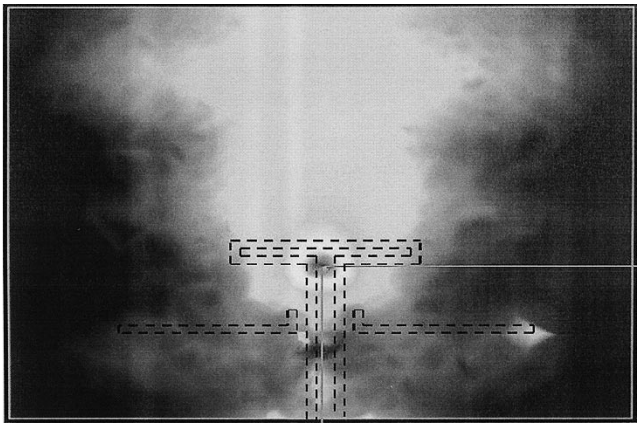

Fig. 6. Reflector-based launcher electric-field distribution at the center of the slab.

is related to the slot initial input impedance $(Z_{\rm slot})$ by the following relation:

$$Z_{\rm in} = \frac{Z_{\rm slot}}{N^2}. \tag{7}$$

Changing the reflector lengths L_R and d enabled matching the input impedance to exactly 50 Ω. However, there is one drawback of using the folded slot. Generally, it was noted that the more folded slots employed, the smaller the bandwidth achieved. Consequently, the designs were optimized to operate with one or two folded slots. Two sets of reflector-based launchers with different dimensions were designed, fabricated, and measured. The first set of launchers was fabricated on a 1.016-mm-thick alumina substrate to operate around 30 GHz. The second set of launchers was fabricated on a 2.54-mm-thick Duroid substrate $(\varepsilon_r = 10.2)$ to operate around 12 GHz. In Section III-A.2, the numerical and experimental results are presented.

Numerical and Experimental Results: The launchers were simulated using both *IE3D*, and *HFSS*. In *IE3D*, the simulation was performed using magnetic current modeling. On the other hand, in *HFSS*, electrical-current-based simulation is performed. The simulation setup was chosen so that the slots are etched onto a large-, but finite-size ground plane placed inside an absorbing-boundary-condition box. The resultant electric-field distribution at the center of the slab using *HFSS* is shown in Fig. 6. It can be deduced from the field distribution that the launcher is directive with more power directed in the forward direction compared to that in the back direction.

To facilitate measurement of the amount of power that is directed in the forward direction compared to that in the backward direction, a different configuration was employed. This new configuration is shown in Fig. 7. It facilitates the testing process as it conforms to the practical setting using a network analyzer. The forward coupling (S_{21}) is measured by the value of the coupling between the launcher under test (port 1) and the launcher connected to port 2, as indicated in Fig. 7. On the other hand, the backward coupling (S_{31}) is measured by the value of the coupling between the launcher under test (port 1) and the launcher connected to port 3. The difference between S_{21} and S_{31} (in decibels) yields the forward/backward directivity

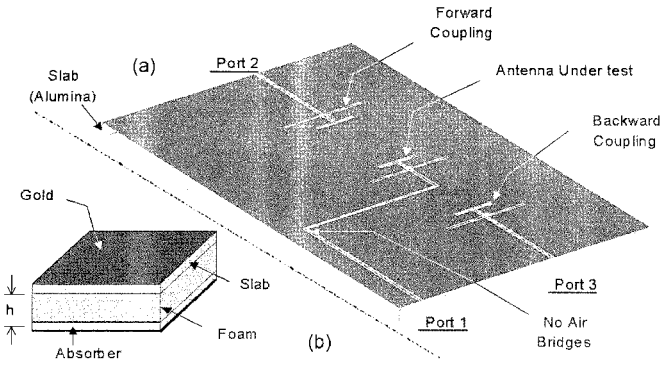

Fig. 7. Simulation and measurement setup for testing the launchers directivities.

TABLE I
DIMENSIONS OF THE REFLECTOR-BASED LAUNCHER OPERATING AT 30 GHz (MICROMETERS)

L_R	L_M	L_S	d	g	t	a	b	N
1864.5	1853	690	200	50	100	50	50	2

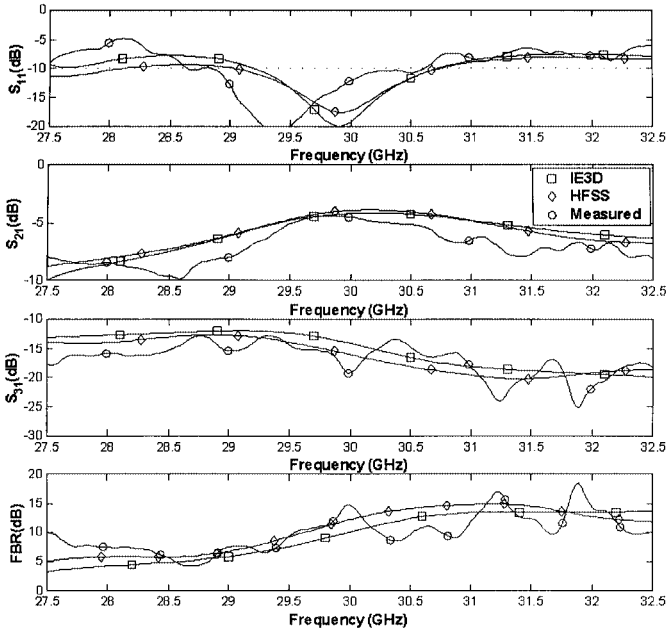

Fig. 8. Reflector-based launcher measured and simulated results.

ratio. The theoretical results obtained based on the use of this arrangement for both *IE3D* and *HFSS* for the reflector-based launcher with the dimensions given in Table I are also shown in Fig. 8. Using *IE3D*, a forward coupling of -4.2 dB is predicted compared to -3.9 dB for *HFSS*. Both simulators show directivity better than 15 dB (FBR), and a -10-dB bandwidth of 1.49 GHz. The close agreement between the results from both simulators, (which are based on two different numerical techniques) provides confidence in the results. The launchers were fabricated and measured. During the measurements, a thick layer of foam ($4\times$ the substrate thickness) and a layer of absorber material were added below the substrate, as shown in Fig. 7(b). The absorber prevented any reflections from the lower ground-plane surface. On the other hand, the foam layer allowed the $\rm TM_0$-mode profile to be satisfied and, hence,

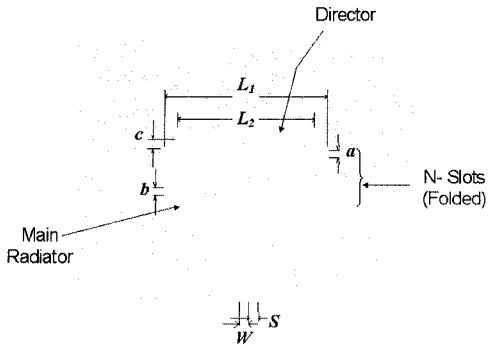

Fig. 9. Configuration of the director-based launcher.

TABLE II
DIMENSIONS OF THE DIRECTOR-BASED LAUNCHER OPERATING AT 12 GHz (MILLIMETERS)

L_1	L_2	a	b	c	W	S	N
5.65	4.72	0.25	0.25	0.25	0.5	0.25	3

allowed the mode to propagate. The measured results are also shown in Fig. 8. A maximum front coupling of −4.4 dB and minimum backward coupling of −19.3 dB were measured with impedance bandwidth of 2 GHz. The maximum measured directivity (FBR) is 14.8 dB at 30 GHz, which is very close to the results obtained from both simulators.

B. Director-Based Launcher

As the name implies, this launcher achieves the directivity using a Yagi–Uda-like director concept. In this structure, the director slot is placed close to the driven slot, forcing an almost 180 ° phase shift between the magnetic currents on both slots. Toward the driven slot, the fields almost completely cancel, forming very low backward field excitation. On the other hand, toward the director, the resultant field does not completely cancel, forming the forward-directed field excitation. As in the case of the reflector-based structure, the ratio between the forward and backward field values yields the launcher directivity. The directivity was maximized by optimizing the length of the director and the spacing between the two slots. The launcher structure is shown in Fig. 9, where use is made of a half-wavelength slot (at the resonance frequency) loaded with a director slot that is slightly shorter. The final optimized dimensions of the director-based quasi-Yagi–Uda launcher built to operate at a center frequency of 11.8 GHz are given in Table II. To match this launcher structure to a 50-Ω system, three slots were used in a folded-slot configuration.

The antenna operates at a center frequency of 11.8 GHz with a (-10-dB) bandwidth of 0.26 GHz (2.2%), and matching better than −30 dB. The simulated and measured results are shown in Fig. 10, where it can be seen that good agreement is obtained. Compared to the reflector-based configuration, the director-based launcher exhibits lower bandwidth. This is a direct result of the relatively large number (3) of the folded slots used in the director-based configuration. On the other hand, the director-based launcher has slightly better directivity performance and occupies less space.

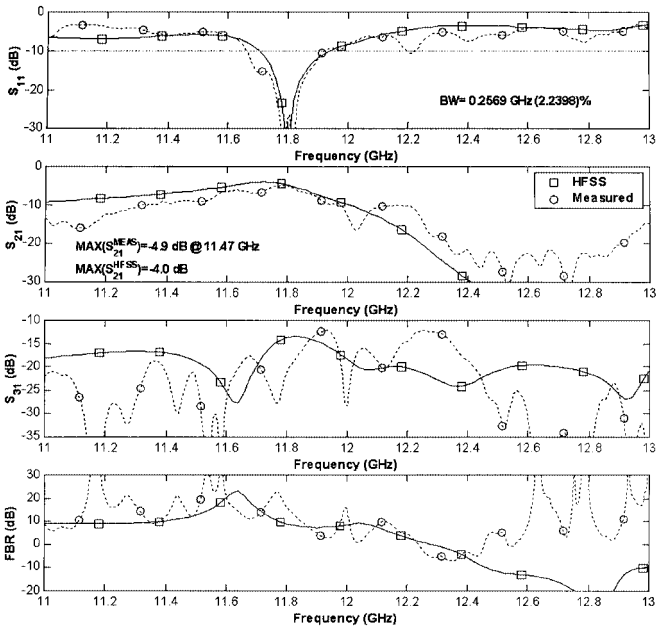

Fig. 10. Director-based launcher measured and simulated results.

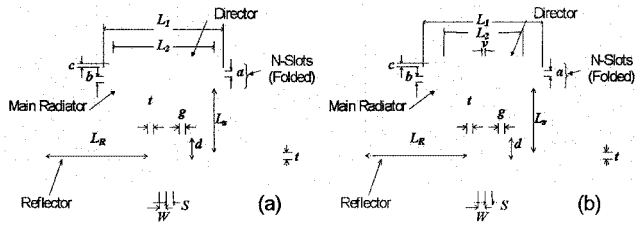

Fig. 11. Configuration of the reflector–director-based launchers.

C. Reflector–Director-Based Launcher

A better front coupling (S_{21}) and directivity could be achieved by combining both the director and reflector; however, optimizing such structure is quite complicated. This is due to the fact that there are too many parameters to be optimized compared to having just a reflector or director. Accordingly, to optimize the full structure, the reflector and director dimensions were optimized separately and then combined. Two possible configurations of the reflector–director-based launcher were examined. The two configurations are shown in Fig. 11. The launcher in Fig. 11(a) employs the director-based configuration presented earlier, while the launcher in Fig. 11(b) employs a modified director-based configuration. The modified director-based structure director is connected directly to the driven slot. The launchers final optimized dimensions are given in Table III. Both launchers were later fabricated on a 2.54-mm-thick Duroid substrate. The simulated and measured results of both configurations are shown in Figs. 12 and 13. The measured results for the launcher in Fig. 11(a) show a maximum forward coupling of −2.9 dB and an impedance bandwidth larger than 0.8 GHz (7.2%). On the other hand, the launcher in Fig. 11(b) yields a maximum forward coupling of −3.5 dB, with an impedance bandwidth of 0.5 GHz (4.2%).

TABLE III
DIMENSIONS OF THE REFLECTOR–DIRECTOR-BASED LAUNCHERS OPERATING AT 12 GHz (MILLIMETER)

Design	L_1	L_2	L_R	L_s	d	t	g	a	b	c	v	W	S	N
(a)	5.65	4.72	4.15	2.25	1.125	0.25	0.25	0.25	0.25	0.25	-	0.5	0.25	2
(b)	6.9	4.72	4.15	0.5	1.125	0.25	0.25	0.25	0.25	0.5	0.25	0.5	0.25	2

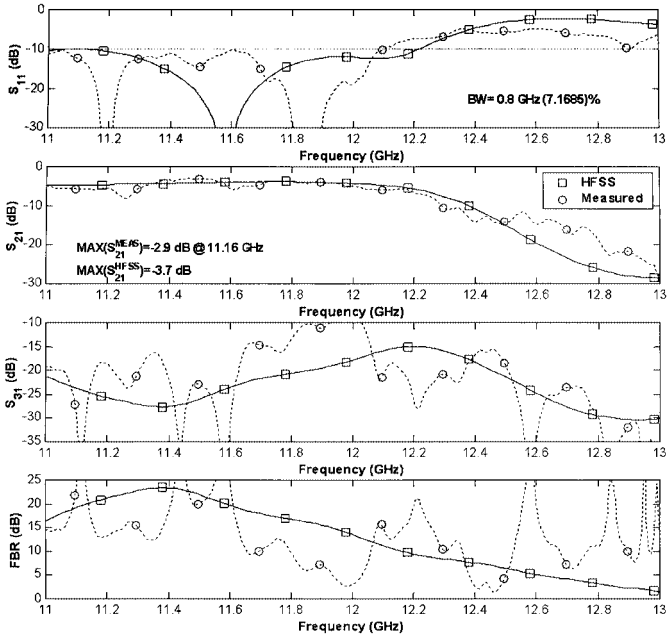

Fig. 12. Measured and simulated results for the reflector–director-based launcher of Fig. 11(a).

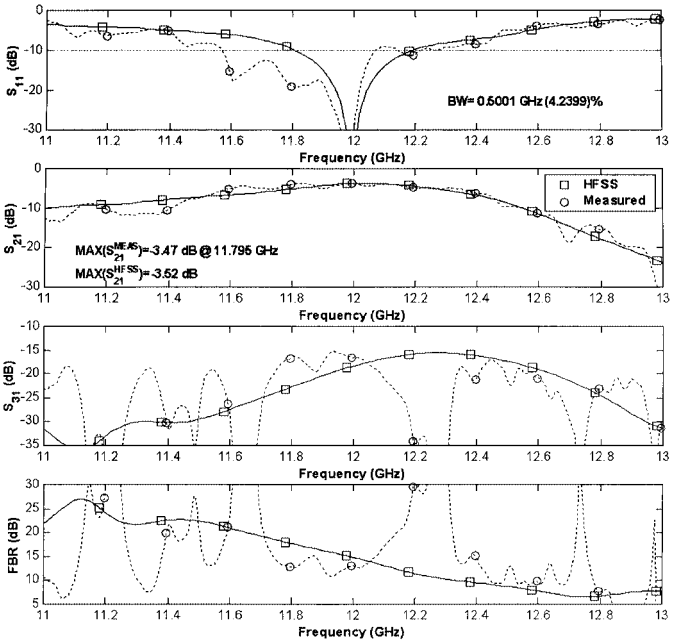

Fig. 13. Measured and simulated results for the reflector–director-based launcher of Fig. 11(b).

IV. CONCLUSION

In this paper, several novel CPW-fed launchers have been presented. These configurations included a reflector-based configuration, director-based configuration, and two reflector–director-based configurations. The realization of the launcher included the optimization of the slab thickness to maximize the surface-wave power excitation. The launchers design was verified both numerically and experimentally. Two sets of launchers were fabricated and measured at two different frequency bands. The launchers have the advantages of being compact and uniplanar, with directivities better than 14.5 dB, and could be useful in the newly developed slab-beam quasi-optical power combiners and other applications.

ACKNOWLEDGMENT

Author S. F. Mahmoud would like to thank Kuwait University, Safat, Kuwait, for granting him sabbatical leave during the 2001–2002 academic year. The authors gratefully acknowledge NORTEL for their valuable help during the experimental phase of this study.

REFERENCES

[1] J. W. Mink and F. K. Schwering, "A hybrid dielectric slab-beam waveguide for the sub-millimeter wave region," *IEEE Trans. Microwave Theory Tech.*, vol. 41, pp. 1720–1729, Oct. 1993.

[2] A. R. Perkons, Y. Qian, and T. Itoh, "TM surface-wave power combining by a planar active-lens amplifier," *IEEE Trans. Microwave Theory Tech.*, vol. 46, pp. 775–783, June 1998.

[3] H. F. Hammad, A. P. Freundorfer, and Y. M. M. Antar, "CPW based 2D lens array for slab-beam power combining array," in *IEEE AP-S North American Radio Science Symp. Meeting*, Salt Lake City, UT, July 2000, pp. 798–801.

[4] J. Harvey, E. R. Brown, D. B. Rutledge, and R. A. York, "Spatial power combining for high-power transmitters," *IEEE Microwave Mag.*, pp. 48–59, Dec. 2000.

[5] T. Rozzi and M. Mongiardo, *Open Electromagnetic Waveguides*, ser. Electromagnetic Waves 43. London, U.K.: IEE Press, 1997.

[6] K. C. Gupta, R. Garg, I. Bahl, and P. Bhartia, *Microstrip Lines and Slotlines*, 2nd ed. Norwood, MA: Artech House, 1996.

[7] Jasik, *Antenna Engineering Handbook*, 1st ed. New York: McGraw-Hill, 1961.

[8] A. A. Oliner, "Types of leaky dominant modes and spectral gaps on printed-circuit lines," in *Directions for the Next Generation of MMIC Devices and Systems*. New York: Plenum, 1997.

[9] M. Tsuji, H. Shigesawa, and A. A. Oliner, "New interesting leakage behavior on coplanar waveguides of finite and infinite widths," *IEEE Trans. Microwave Theory Tech.*, vol. -39, pp. 2130–2137, Dec. 1991.

[10] N. Alexopoulos, P. B. Katehi, and D. B. Rutledge, "Substrate optimization for integrated circuit antennas," *IEEE Trans. Microwave Theory Tech.*, vol. MTT-31, pp. 550–557, July 1983.

[11] S. F. Mahmoud, Y. M. M. Antar, and H. F. Hammad, "Optimum excitation of surface waves on a planar structure," presented at the URSI Int. Electromagnetic Theory Symp., Maastricht, The Netherlands, Aug. 2002.

[12] S. F. Mahmoud, Y. M. M. Antar, H. F. Hammad, and A. P. Freundorfer, "Theoretical consideration in the optimization of surface waves on a planar structure," *IEEE Trans. Antennas Propagat.*, submitted for publication.

[13] H. F. Hammad, S. F. Mahmoud, Y. M. M. Antar, and A. P. Freundorfer, "Optimization of surface waves on a grounded dielectric slab by a slot antenna," in *IEEE AP-S North American Radio Science Symp. Meeting*, San Antonio, TX, pp. 602–605.

[14] H. F. Hammad, Y. M. M. Antar, and A. P. Freundorfer, "A uni-planar slot antenna for TM slab mode excitation," *Electron. Lett.*, pp. 1500–1501, Dec. 2001.

[15] S. S. Sierra-Garcia and J. J. Laurin, "Study of a CPW inductively coupled slot antennas," *IEEE Trans. Antennas Propagat.*, vol. 47, pp. 58–64, Jan. 1999.

[16] H. S. Tsai, M. J. W. Rodwell, and R. A. York, "Planar amplifier array with improved bandwidth using folded-slots," *IEEE Microwave Guided Wave Lett.*, vol. 4, pp. 112–114, Apr. 1994.

Hany F. Hammad received the B.Sc. degree (with honors) from Ain Shames University, Cairo, Egypt, in 1994, and the M.Sc. and Ph.D. degrees from Queen's University, Kingston, ON, Canada, in 1997 and 2002, respectively.

His research interests are the analysis and design of antennas and microwave integrated circuits.

Dr. Hammad's thesis was ranked as the "Outstanding Thesis of Engineering and Applied Science Division" at Queen's University.

Yahia M. M. Antar (S'73–M'76–SM'86–F'00) was born on November 18, 1946, in Meit Temmama, Egypt. He received the B.Sc. (with honors) degree from Alexandria University, Alexandria, Egypt, in 1966, and the M.Sc. and Ph.D. degrees from the University of Manitoba, Winnipeg, MB, Canada, in 1971 and 1975, respectively, all in electrical engineering.

In 1966, he joined the Faculty of Engineering, Alexandria University, where he was involved in teaching and research. From 1976 to 1977, he was with the Faculty of Engineering, University of Regina. In June 1977, he was awarded a Visiting Fellowship from the Government of Canada to work with the Communications Research Centre, Department of Communications, Shirley's Bay, Ottawa, ON, Canada, where he was involved in research and development of satellite technology with the Space Electronics Group. In May 1979, he joined the Division of Electrical Engineering, National Research Council of Canada, Ottawa, ON, Canada, where he was involved with polarization radar applications in remote sensing of precipitation, radio wave propagation, electromagnetic scattering, and radar cross-sectional investigations. In November 1987, he joined the staff of the Department of Electrical and Computer Engineering, Royal Military College of Canada, Kingston, ON, Canada, where he is currently a Professor of electrical and computer engineering. He holds an adjunct appointment at the University of Manitoba, and has a cross appointment with Queen's University, Kingston, ON, Canada. He has authored or coauthored over 100 journal papers on these topics, and has supervised or co-supervised over 45 Ph.D. and M.Sc. theses at the Royal Military College and Queen's University, of which three have received the Governor General Gold Medal. His current research interests include polarization studies, integrated antennas, and microwave and millimeter-wave circuits.

Dr. Antar is the chairman of the Canadian National Commission (CNC, URSI). Dr. Antar is an associate editor (features) of the *IEEE Antennas and Propagation Magazine*. In May 2002, he became the Holder of a Canada Research Chair (CRC) in applied electromagnetics and microwave engineering. He was the recipient of a University Fellowship of the University of Manitoba and a National Research Council (NRC) Postgraduate Fellowship and Post-Doctoral Fellowship.

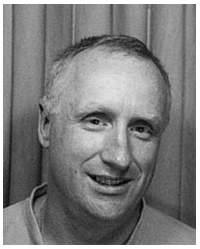

Al P. Freundorfer (S'80–M'82) received the B.A.Sc., M.A.Sc., and Ph.D. degrees from the University of Toronto, Toronto, ON, Canada, in 1981, 1983, and 1989, respectively.

In 1990, he joined the Department of Electrical Engineering, Queen's University, Kingston, ON, Canada, where he has been involved with nonlinear optics of organic crystals and coherent optical network analysis, as well as microwave integrated circuits. He is currently focused on monolithic microwave circuits used in lightwave systems with bit rates in excess of 20 Gb/s and on monolithic millimeter-wave integrated circuits used in wireless communications.

Samir F. Mahmoud (S'69–M'73–SM'83) received the B.Sc. degree in electronic engineering from Cairo University, Cairo, Egypt, in 1964, and the M.Sc. and Ph.D. degrees in electrical engineering from Queen's University, Kingston, ON, Canada in 1970 and 1973, respectively.

During the 1973–1974 academic year, he was a Visiting Research Fellow with the Cooperative Institute for Research in Environmental Sciences (CIRES), Boulder, CO, during which time he performed research on communication in tunnels. He spent two sabbatical years (1980–1982) with Queen Mary College, London, U.K., and British Aerospace, Stevenage, U.K., here he was involved in the design of antennas for satellite communication. He is currently a Full Professor with the Electrical Engineering Department, Kuwait University, Safat, Kuwait. He has recently visited several places, including the Interuniversity Micro-Electronics Centre (IMEC), Leuven, Belgium, and spent a sabbatical leave with Queen's University, and the Royal Military College, Kingston, ON, Canada, in 2001–2002. His research activities have been in the areas of antennas, geophysics, tunnel communication, electromagnetic wave interaction with composite materials, and microwave integrated circuits.

Dr. Mahmoud is a Fellow of the Institution of Electrical Engineers (IEE), U.K. He was the recipient of the 2003 Microwave prize of the IEEE Microwave Theory and Techniques Society (IEEE MTT-S).